conditions, is therefore

$$\mathrm{Eff}(z_{\mathrm{opt}}) = \frac{|V_2(z_{\mathrm{opt}})|^2}{V_1^2(0)} \times 100\% = \{(0.37) Q_2 K_N V_1(0)\}^2 \times 100\% \quad (27)$$

which is seen to be proportional to $(Q_2 K_N)^2$.

III. Conclusion

According to the simple small-signal theory presented above, the largest SHG of a relatively low-loss transmission line will occur when the transmission line satisfies both the *coherence* condition

$$z_l < (z_c/4) \quad (28)$$

and the *optimum length* condition

$$(\beta_2 z_l) = 2Q_2. \quad (29)$$

Further, the maximum obtainable SHG is seen to be proportional to the square of the $(Q_2 K_N)$ product. Accordingly, tradeoffs between the "transmission Q" and the "nonlinearity factor" may be possible which will maximize this product for a particular line implementation. The simple theory also shows that conversion efficiency is proportional to the square of the input voltage. Note, however, that (27) assumes $|V_2| \ll |V_1|$ and that third- and higher order terms in the Taylor's series expansion of (1) have been systematically ignored. Thus, this result can be rigorously justified only for small input signals satisfying

$$V_1(0) \ll \{3q''/q'''\}. \quad (30)$$

References

[1] See, e.g., J. W. Archer, "Millimeter wavelength frequency multipliers," *IEEE Trans. Microwave Theory Tech.*, vol. MTT-29, p. 552, June 1981.

[2] See, e g, K. S Champlin and G. Eisenstein, "Cut-off frequency of submillimeter Schottky barrier diodes," *IEEE Trans. Microwave Theory Tech.*, vol. MTT-26, pp. 31–34, Jan. 1978

[3] V P Popov and T. A Bickart, "*RC* transmission line with nonlinear controlled parameters—Small-signal characteristics," *IEEE Trans. Circuits Syst.*, vol. CAS-21, pp. 268–270, Mar. 1974

[4] V. P Popov and T A. Bickart, "*RC* transmission line with nonlinear resistance: Large-signal response computation," *IEEE Trans Circuits Syst.*, vol. CAS-21, pp. 666–671, Sept. 1974.

[5] K Everszumrode, B. Brockmann, and D Jager, "Efficiency of harmonic frequency generation along schottky contact microstrip lines," *Arch. Elek. Übertragung.*, vol. 31, pp. 212–215, 1977.

[6] D. Jager *et al.*, "Bias-dependent small-signal parameters of Schottky contact microstrip lines," *Solid-State Electron.*, vol. 17, pp. 777–783, 1974.

[7] H. Hasegawa *et al.*, "Properties of microstrip line on Si-SiO_2 systems," *IEEE Trans. Microwave Theory Tech.*, vol MTT-19, pp. 869–881, Nov. 1971.

[8] H Hasegawa *et al*, "Slow-wave propagation along a microstrip line on Si-SiO_2 systems," *Proc. IEEE*, vol. 59, pp. 297–299, Feb. 1971.

[9] G W. Hughes, "Microwave properties of nonlinear MIS and Schottky barrier microstrip," *IEEE Trans. Electron Devices*, vol Ed-22, pp. 945–956, 1975.

[10] D Jager, "Slow wave propagation along variable Schottky contact microstrip line," *IEEE Trans Microwave Theory Tech.*, vol MTT-24, pp 566–573, Sept. 1976.

[11] H. Hasegawa and H. Okizaki, "MIS and Schottky slow-wave coplanar striplines on GaAs substrates," *Electron. Lett*, vol. 13, pp. 663–664, 1977

[12] S. Seki and H Hasegawa, "Cross tie slow-wave coplanar waveguide on semiinsulating GaAs substrates," *Electron Lett*, vol. 17, pp 940–951, 1981.

[13] Y. Shih and T Itoh, "Analysis of printed transmission lines for monolithic integrated circuits," *Electron. Lett*, vol. 18, pp. 589–590, 1982.

[14] Y Fukuoka and T Itoh, "Analysis of slow-wave phenomena in coplanar waveguide on a semiconductor substrate," *Electron. Lett.*, vol. 18, pp. 589–590, 1982.

[15] R Sorrentino *et al.*, "Characteristics of metal-insulator-semiconductor coplanar waveguides for monolithic microwave circuits," *IEEE Trans. Microwave Theory Tech.*, vol. MTT-32, pp. 410–416, Apr., 1984.

Transient Analysis of a Directional Coupler Using a Coupled Microstrip Slot line in Three-Dimensional Space

SHOICHI KOIKE, NORINOBU YOSHIDA, AND ICHIRO FUKAI

Abstract **— In recent MIC techniques, double-sided MIC has been studied because its advantages in propagation characteristics are greater than that of conventional MIC's. A coupled microstrip slotline is one of them. Its application to various circuit elements has often been discussed. But the coupled microstrip slotline is essentially three-dimensional structure, so the analysis demands a rigorous three-dimensional treatment. Also, the recent high-speed pulse technique demands analysis in the time domain. The present paper treats a directional coupler using the coupled microstrip slotline in three-dimensional space and time. The results of the directional coupler analysis is presented with the complicated time variation of the three-dimensional electromagnetic field. So, the mechanism of the directional coupling phenomena that is produced by the propagation characteristics of the even and odd modes is presented in the time domain. In particular, the instantaneous diagram of the Poynting vector details the energy flow in the transient process. For the analysis of the characteristics of the complex microwave device, these results present the utilities of the various field distributions that are obtained by the three-dimensional vector analysis in the time domain.**

I. Introduction

In recent MIC techniques, a double-sided MIC has been studied extensively because of its advantages in propagation characteristics over the conventional MIC. A coupled microstrip slotline is one of the fundamental structures of the double-sided MIC. The structure is as follows: the stripline is on one side of the dielectric substrate and the slotline is on the other side. The coupled stripline slotline has properties that the dispersion characteristics and the characteristic impedance are controlled sensitively and extensively by changing the geometrical dimension. The design of the directional coupler by use of the microstrip slotline was proposed by F. C. de Ronde in 1970, [1] its theoretical consideration was given by B. Schiek, [2], [3], the synthetic method of the design and experimental results were performed by H. Ogawa, [4], [5], and the design with compensation slotlines and the comparison with the experiment were presented by R. K. Hoffmann [6], [7]. The conventional MIC based on the stripline has been treated by a two-dimensional analysis. But, the coupled microstrip slotline is essentially a three-dimensional structure, so the analysis demands a rigorous three-dimensional treatment. Also, the recent development of high-speed pulse techniques demands the analysis in the time domain. The transient analysis of the electromagnetic field is not only useful in clarifying the field response but also yields information on the mechanism by

Manuscript received June 18, 1985; revised October 18, 1985.

The authors are with the Faculty of Engineering, Hokkaido University, Sapporo, 060 Japan.

IEEE Log Number 8406856.

0018-9480/86/0300-0353$01.00 ©1986 IEEE

which the distribution of the electromagnetic field in the stationary state is brought about [8]–[10]. As a time-domain analysis method for a three-dimensional electromagnetic field, we have proposed a method by the nodal equations that formulate the equivalent circuit which simulate Maxwell's equations by Bergeron's method [11]. (This is referred to as the present method.) It has been shown that the present method uses all of the electromagnetic fields, and the boundary and medium conditions are represented three-dimensionally by equivalent circuits. Therefore, the present method is useful for formulation of the problem described above in which a complicated boundary shape and dielectric materials are included. The present paper treats a directional coupler using the coupled microstrip slotline in three-dimensional space and time. The mechanism of the directional coupling phenomena that is produced by the propagation characteristics of the even and odd modes is presented in time domain. In particular, the instantaneous diagram of the Poynting vector details the energy flow in transient process. For complex microwave device characteristics, these results present the utilities of the various expressions of the field distributions that are obtained by three dimensional vector analysis in time domain.

II. Analyzed Model of the Directional Coupler

Fig. 1 shows the model of the directional coupler using the coupled microstrip slotline. In this analysis, the conductor is supposed to have infinite conductivity and the dielectric constant of the substrate: ϵ_s is chosen to be 9.6. In this figure, Δd is the interval between adjacent nodes in the equivalent circuit. The period T of the sinusoidal incident wave is $290\Delta t$, where Δt is the time interval between iterations and corresponds to the propagation time between the adjacent nodes in the equivalent circuit. In a three-dimensional equivalent circuit, the correspondence between the division of the period and of the plane wavelength in free space are $2n\Delta t$ and $n\Delta d$ because of their slow-wave characteristics [12]. So, in this analysis, the wavelength in free space is $145\Delta d$. When $1\Delta d$ is assumed to be 0.075 mm, the frequency becomes approximately $f = 27.6$ GHz and the thickness of the dielectric substrate becomes $d = 0.3$ mm. If all space is filled with dielectric ($\epsilon_s = 9.6$), the wavelength becomes $46.8\Delta d$. It is generally known that the number of the divisions of the period and the wavelength should be more than ten in the difference formulation. Therefore, the division number of the period and wavelength in this analysis are sufficient for good resolution in time and space.

III. Analyzed Results and Discussion

A. Characteristic Impedance and Effective Dielectric Constant of Coupled Strip Slotline

In order to design the directional coupler, we must know the effect of the geometrical parameter of the coupled strip slotline. So the values of the characteristic impedance Z and effective dielectric constant ϵ_{eff} must be estimated as the parameters, such as the width of the strip and the width of the slot. Fig. 2 shows the calculated results of the characteristic impedance and the effective dielectric constant of the coupled strip slotline for the above conditions. The width of the strip and the slot are normalized to d, and expressed as $2w/d$ and $2t/d$, respectively. For the even mode, the calculated values of the characteristic impedance Z_{even} (○ in Fig. 2) and the effective dielectric constant $\epsilon_{\text{eff, even}}$ (●) are plotted as a function of the width of the slot $2t/d$ for the parameter of the width of the strip $2w/d = 1$. For the odd mode, the calculated values of the characteristic impedance Z_{odd} (△) and the effective dielectric constant $\epsilon_{\text{eff, odd}}$ (▲) are plotted as a function of the width of the strip $2w/d$ for the parameter of the width of the slot $2t/d = 0.5$. Definitions of Z_{even}, Z_{odd} in [4] are used. The effective dielectric constant is evaluated from the ratio of the propagation wavelength in free space λ_0 to that in the coupled line λ_g. In the figure, the computed results are connected with curves for ease of viewing. To verify the validity of our computed results, the analytical results are also plotted. For the even mode, the analytical results of the stripline with no slot ($2t/d = 0$) are plotted [13], [14], and for the odd mode, the analytical results of the slotline with no strip ($2w/d = 0$) are plotted [15]. These analytical results are expressed by the symbols " $>$ " and " $<$ ", respectively. It is shown that both results agree well.

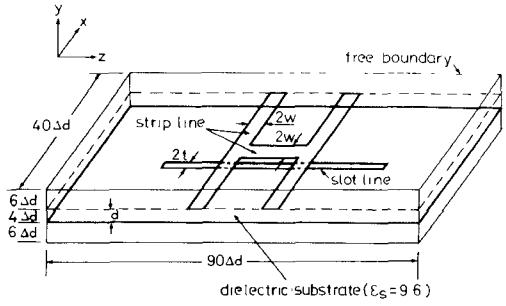

Fig. 1. Model of directional coupler using the microstrip slotline.

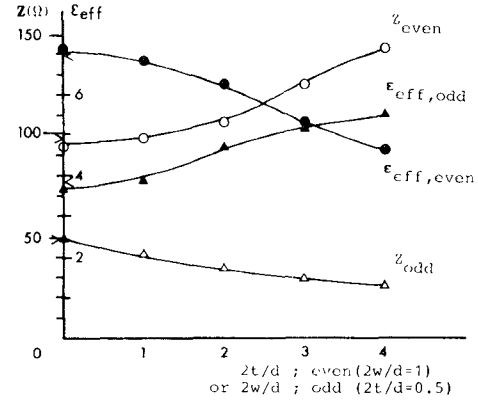

Fig 2 Characteristic impedance and effective dielectric constant of coupled microstrip slotline ($\epsilon_s = 9.6$, $f = 27.6$ GHz).

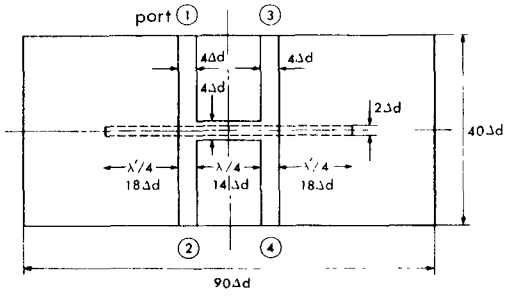

Fig. 3 Ground plan of directional coupler.

B. Directional Coupler

The coupling k of the directional coupler is given by

$$k = \frac{Z_{\text{even}} - Z_{\text{odd}}}{Z_{\text{even}} + Z_{\text{odd}}}. \tag{1}$$

The coupling for $2w/d = 1$ and $2t/d = 0.5$ is estimated as 7.7 dB

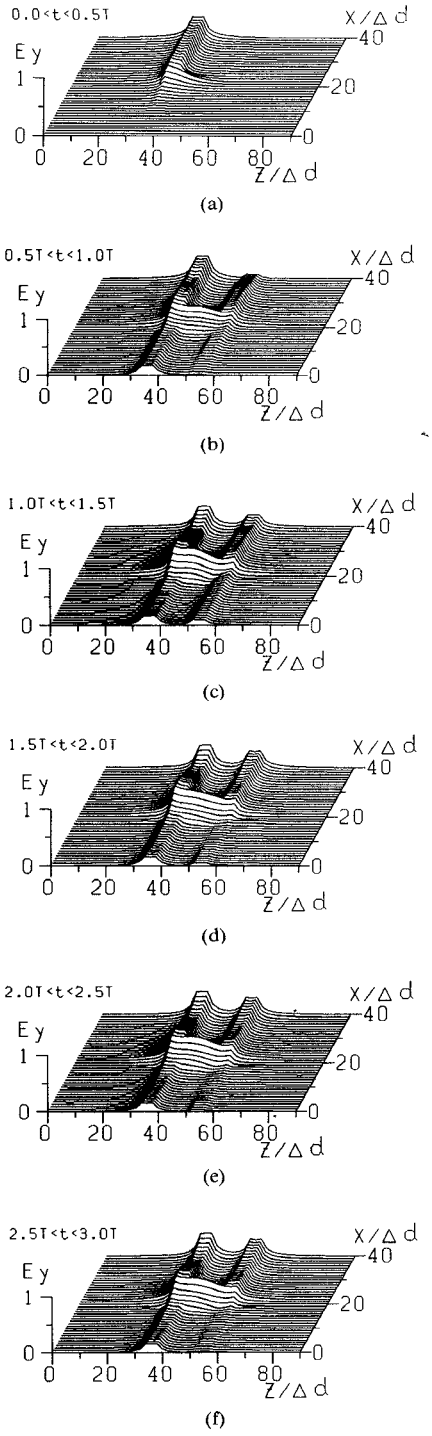

Fig 4 Time variations of the spatial distribution of the electric field E_y beneath Δd from the strip conductor for the directional coupler.

using the values of the impedance in Fig. 2. For the number of divisions in the present analysis, the width of the strip $2w/d = 1$ and width of the slot $2t/d = 0.5$ are limited by the memory size of the computer used. Fig. 3 shows the geometrical parameter of the ground plan of the analyzed directional coupler in Fig. 1. $\lambda/4$ is $14\Delta d$ from the value of the $\epsilon_{\text{eff, even}}$ in Fig. 2. $\lambda/4$ is $18\Delta d$ from the value of the $\epsilon_{\text{eff, odd}}$ in Fig. 2. In this analysis, we choose the same width for the four feeding lines and for the strip of the microstrip-slot-coupling sections. So, this unmatched condition at the four ports causes the decrease of the directivity and also the increase of the insertion loss between the input port 1 and isolated port 4. The time variation of the spatial distribution of the electric field E_y for the sinusoidal voltage wave applied from port 1 is shown in Fig. 4. The xz-plane we observed is $1\Delta d$ beneath the strip conductor. The initial time $t = 0$ corresponds to the incidence of the wave at port 1. At this time, all components of the electromagnetic field are assumed to be zero. The expressions in the figures such as $0 < t < 0.5T$ are the time intervals used for finding the maximum value at each point to provide the spatial distributions rather than the instantaneous values. At the time interval $0 < t < 0.5T$, the wave applied from port 1 begins to part to port 2 in the x-direction and to the coupled strip slotline in the z-direction. At $0.5T < t < 1.0T$, the amplitude of the wave along the sides of ports 1 and 3 of that part of the coupled line is larger than that of the opposite side. It is considered that these conditions are caused by the addition of the even and odd modes. These modes are generated by the incident wave at that part of the coupled line. But the electric field of the odd mode generated by the slot is weak, so the wave propagates to the branch of port 4. The wave reaches port 2 because the strip between ports 1 and 2 is orthogonal to the slot and the influence of the slot is small. Also, the composed wave of the even and odd modes reaches port 3. The amplitude of the field decreases smoothly in the open terminal of that part of the slot $\lambda/4$. The electric field of the odd mode gradually increases in time, so the wave arriving at port 4 gradually decreases, as shown in Fig. 4(c)–(f). At $2.5T < t < 3.0T$, the distribution of the field is almost regarded as steady-state distributions because, after this time, the field distribution hardly changes. The wave arriving at port 4 is close to zero. So the characteristics of the directional coupler are realized in the steady state. But in the transient state, the characteristics of the isolation between each port is not complete, so, for the high-speed pulse wave, these transient phenomena give a bad performance. In the steady state, the ratio of the amplitude of the wave at port 1 to that at port 2 is about 7.7 dB. The resultant value agrees well with the preceding ones derived from (1) using he values of the impedance in Fig. 2.

Fig. 5 shows the time variation of the instantaneous distribution of the electric field E_y. The observed plane is the same as in Fig. 4. The instantaneous values of the electric field E_y are observed at intervals of $T/4$ from $t = 0$ to $t = 3T$. These figures show the successive stages of the transient wave, and each figure can be interpreted as follows: At $t = T/4$, the wave has not yet reached the coupled strip slotline. At $t = 2T/4$, the field begins to part to the coupled strip slotline in the z-direction and to port 2 in the x-direction, but the distinct change of wave form due to the influence of the slot is not visible. At $t = 3T/4$, the wave decreased by the slot propagates to port 2, and the wave is also propagation in the z-direction along the coupled line. The large amplitude part of the wave at the sides of ports 1 and 3 begins to propagate to port 3 and the small amplitude part of the wave at the sides of ports 2 and 4 begins to propagate to port 4. At $t = 4T/4$, the wave reaches ports 2, 3, and 4. At $t = 5T/4$, $6T/4$, $\cdots$, and $12T/4$, the sinusoidal changing of the field in time continues, but the field at port 4 has gradually decreased. At the final time step, the field pattern almost shows a steady-state situation.

Fig. 6 shows time variations of the instantaneous Poynting vector. The observed plane is the same as in the previous figures. The length and the direction of the arrow correspond to the magnitude and the direction of the Poynting vector, respectively. The variations of the Poynting vector correspond to the instantaneous field distribution in Fig. 5, so only the attractive patterns of the initial stage of the transient process are presented. The

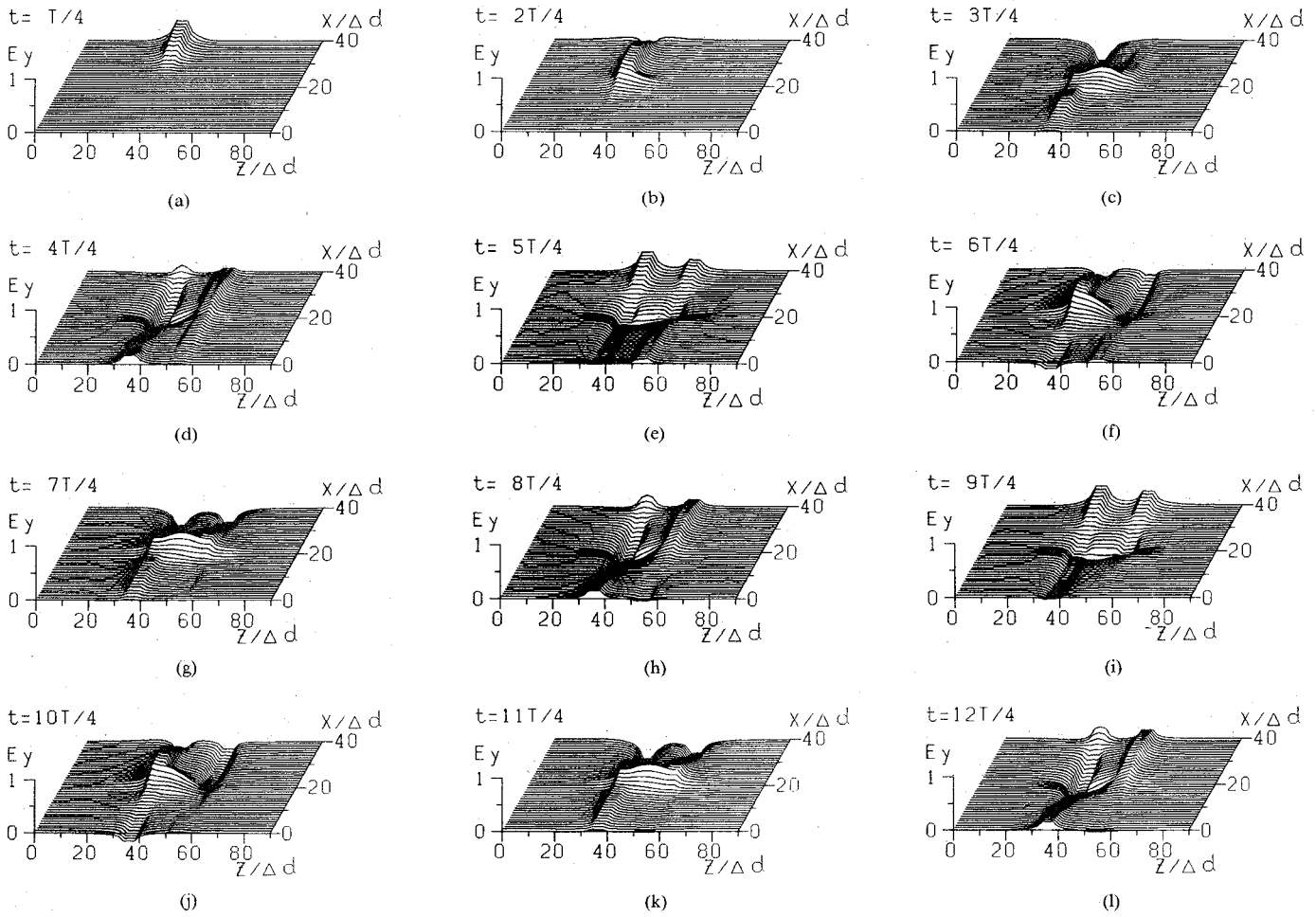

Fig. 5. Time variations of the instantaneous distribution of the electric field E_y beneath Δd from the strip conductor for the directional coupler.

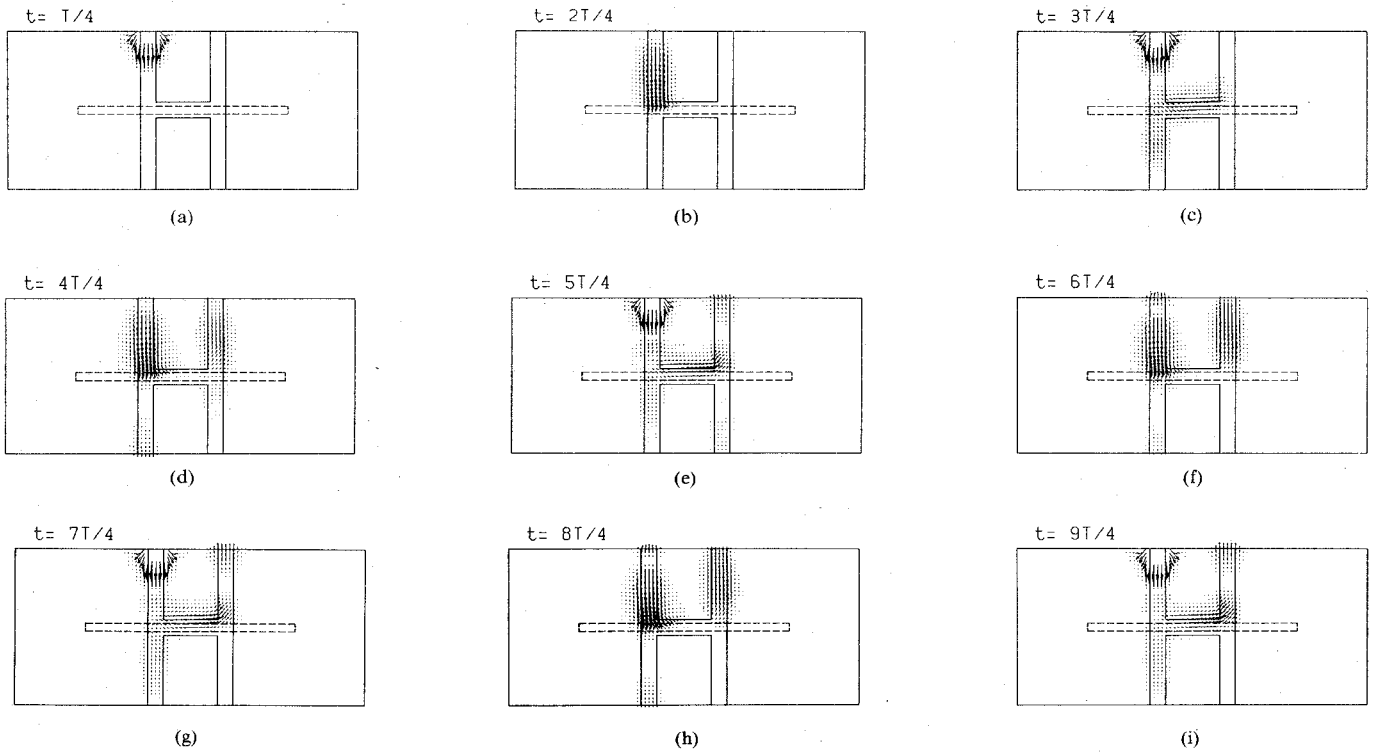

Fig. 6. Time variations of the instantaneous Poynting vector beneath Δd from the strip conductor for the directional coupler.

direction of the Poynting vector shows more clearly transient characteristics of the directional coupler by presenting the pattern of the flow of the electromagnetic energy.

IV. Conclusion

The time variation of electromagnetic fields can be described in two ways. Either the instantaneous distribution is shown or the spatial distribution obtained by taking the envelope of the maximum value during the observation time interval is shown. Using the former method, for example, the detailed propagation characteristics such as the phase and the amplitude of the coupled microstrip slotline at each mode is known. Using the latter method, the process by which the stationary property of the directional coupler is brought about can be known. Also, the expression of the time variation of the instantaneous distribution and the Poynting vector shows more clearly the transient characteristics of the complicated circuit elements, such as the directional coupler. These can be realized by using all electromagnetic components. As shown in this paper, this condition is satisfied by the present method.

In addition, we can easily study the time variations of field in the case of pulse waves where the analysis of the transient phenomena is very important. More analysis is needed for when the size of the slot becomes less, Z_{even} increases, and Z_{odd} decreases, so that a higher coupling directional coupler can be obtained. This subject and results of the pulse wave analysis will be reported in a later paper.

References

[1] F. C. de Ronde, "A new class of microstrip directional coupler," *IEEE Trans Microwave Theory Tech.*, vol. MTT-18, pp. 184–186, May 1970.

[2] B. Schiek, "Hybrid branch line couplers—A useful class of directional couplers," *IEEE Trans. Microwave Theory Tech.*, vol. MTT-22, pp. 864–869, Oct. 1974.

[3] B. Schiek and J. Köhler, "Improving the isolation of 3-dB couplers in microstrip-slotline technique," *IEEE Trans. Microwave Theory Tech.*, vol. MTT-26, pp. 5–7, Jan. 1978.

[4] H. Ogawa, T. Hirota, and M. Aikawa, "Coupled microstrip-slotline directional coupler," *Trans.IECE Japan*, vol. J65-B, pp. 882–889, July 1982.

[5] M Aikawa, "Microstrip line directional coupler with tight coupling and high directivity," *Trans IECE Japan*, vol. J60-B, pp. 253–259, Apr. 1977.

[6] R. K. Hoffmann and J. Siegl, "Microstrip-slot coupler design—Part I: S-parameters of uncompensated and compensated couplers," *IEEE Trans. Microwave Theory Tech.*, vol. MTT-30, pp 1205–1210, Aug. 1982.

[7] R. K. Hoffmann and J. Siegl, "Microstrip-slot coupler design—Part II: Practical design aspects," *IEEE Trans. Microwave Theory Tech.*, vol. MTT-30, pp. 1211–1216, Aug. 1982.

[8] S. Koike, N. Yoshida, and I. Fukai, "Transient analysis of microstrip gap," *Electron. Commun. Japan*, vol. 67-B, pp. 76–83, Nov. 1984.

[9] S. Koike, N. Yoshida, and I. Fukai, "Transient analysis of microstrip gap in three-dimensional space," *IEEE Trans. Microwave Theory Tech.*, vol. MTT-33, pp. 726–730, Aug 1985.

[10] S. Koike, N. Yoshida, and I. Fukai, "Transient analysis of coupled microstrip-slotline," *Trans. IECE Japan*, vol. J68-B, pp. 811–818, July 1985.

[11] N. Yoshida and I. Fukai, "Transient analysis of a stripline having a corner in three-dimensional space," *IEEE Trans. Microwave Theory Tech.*, vol. MTT-32, pp. 491–498, May 1984.

[12] S Akhtarzad and P. B Johns, "Solution of Maxwell's equations in three space dimensions and time by the t.l.m. method of numerical analysis," *Proc. Inst. Elec. Eng.*, vol. 122, pp. 1344–1348, Dec. 1975.

[13] T. Itoh and R. Mittra, "Spectral-domain approach for calculating the dispersion characteristics of microstrip lines," *IEEE Trans. Microwave Theory Tech.*, vol. MTT-21, pp. 496–499, July 1973

[14] H. A. Wheeler, "Transmission-line properties of a strip on a dielectric sheet on a plane," *IEEE Trans. Microwave Theory Tech* , vol. MTT-25, pp. 631–647, Aug. 1977.

[15] S. B. Cohn, "Slot line on a dielectric substrate," *IEEE Trans. Microwave Theory Tech.*, vol. MTT-17, pp. 768–778, Oct. 1969.

Focused Heating in Cylindrical Targets—Part II

JAMES R. WAIT, FELLOW, IEEE, AND MIKAYA LUMORI

***Abstract*—We implement the analytical formulation for the local power dissipated in a conductive target of cylindrical form that was described in Part I. The scheme employs a number N of horn apertures arranged around the periphery of the target. We show sample results for the radial and the azimuthal variations of the normalized local power. The cases where the array is focused at both the center of the target and where it is focused at an eccentric point are considered for $N = 4$, 8, and 16. It is shown that the unwanted secondary "hot spots" can be eliminated if the number N of horn apertures is increased sufficiently. The results are relevant to microwave thermic heating in cancer therapy.**

I. Introduction

The formulation given in a previous communication on focused heating [1] in a cylindrical conductor has now been implemented numerically. The scheme involves placing N aperture sources around the periphery of the target. In our example here, we have chosen $N = 4$, 8, and 16. The formulation follows that in Part I, but we now normalize the results for the purpose of graphical presentation. Finally, we draw some general conclusions about the nature of electromagnetic heating in hyperthermia.

II. Description of the Model

The assumed geometry of the configuration is purely two dimensional, as described quite fully in Part I. The cylindrical target of radius a is homogeneous with conductivity σ, permittivity ϵ, and the free-space permeability μ_0. The horn apertures are disposed around the periphery, arranged so that no gaps exist between them. As indicated in [1, fig. 1] the center of each aperture is located at $\phi_n = n\pi/N$, where $n = 0,1,2,\cdots N-1$.

Because of the assumed polarization of the excitation, the electric field in the target has only an axial or z component, which is written conveniently in the form

$$E_z(\rho,\phi) = \sum_{n=0}^{N-1} E_{z,n}(\rho,\phi).$$

Here

$$E_{z,n}(\rho,\phi) = \Delta_n e^{i\delta_n} \sum_{m=-\infty}^{+\infty} A_m I_m(\gamma\rho)\, e^{-im(\phi-\phi_n)}$$

is the field produced by the nth aperture, where A_m is a coefficient, $I_m(\gamma_\rho)$ is the modified Bessel function of argument $\gamma\rho$, and γ is the complex propagation constant of the homogeneous interior of the target. We recall that $\gamma = [i\mu_0\omega(\sigma + i\epsilon\omega)]^{1/2}$ for a time factor $\exp(i\omega t)$.

Each aperture is assumed to have the same field distribution (as a function of ϕ), but the relative amplitude Δ_n and phase δ_n of each aperture are controllable. For the results presented here, we assume that the horn apertures are in direct contact with the target (i.e., $b = a$ in [1, fig. 1]). Thus, we can write

$$A_m = \frac{1}{2\pi I_m(\gamma a)} \int_{-\pi/N}^{\pi/N} E_{z,0}(a,\phi)\, e^{im\phi}\, d\phi$$

where $E_{z,0}(a,\phi)$ is the aperture illumination over the reference

Manuscript received May 17, 1985, revised October 21, 1985.

The authors are with the Electromagnetics Laboratory, Department of Electrical and Computer Engineering, University of Arizona, Tucson, AZ 85721.

IEEE Log Number 8406857.

0018-9480/86/0300-0357$01.00 ©1986 IEEE